ELSEVIER Nuclear Instruments and Methods in Physics Research A 467–468 (2001) 1318–1321

NUCLEAR INSTRUMENTS & METHODS IN PHYSICS RESEARCH Section A

www.elsevier.com/locate/nima

Iodine imaging in thyroid by fluorescent X-ray CT with 0.05 mm spatial resolution

T. Takeda[a,*], Q. Yu[a,b], T. Yashiro[a], T. Zeniya[a,b], J. Wu[a], Y. Hasegawa[b], Thet-Thet-Lwin[a], K. Hyodo[c], T. Yuasa[b], F.A. Dilmanian[d], T. Akatsuka[b], Y. Itai[a]

[a] *Institute of Clinical Medicine, University of Tsukuba, 1-1-1 Tennoudai, Tsukuba, Ibaraki 305-8575, Japan*
[b] *Faculty of Engineering, Yamagata University, Yonezawa, Yamagata 992-8510, Japan*
[c] *Institute of Materials Structure Science, High Energy Accelerator Research Organization, Tsukuba, Ibaraki 305-0810, Japan*
[d] *Medical Department, Brookhaven National Laboratory, Upton, NY 11973, USA*

Abstract

Fluorescent X-ray computed tomography (FXCT) at a 0.05 mm in-plane spatial resolution and 0.05 mm slice thickness depicted the cross sectional distribution of endogenous iodine within thyroid. The distribution obtained from the FXCT image correlated closely to that obtained from the pathological pictures.

PACS: 07.85.Q; 07.85.T; 78.70.E; 87.62; 87.59.F

Keywords: Fluorescent X-ray computed tomography; Synchrotron radiation; Thyroid; Hyperthyroidism

1. Introduction

Fluorescent X-ray technique is usually used to evaluate very low contents of specific elements in the order of picograms, however, planar-mode fluorescent imaging does not provide any depth information [1]. Using synchrotron X-rays (SR), fluorescent X-ray tomography using small detector [2–4] and fluorescent X-ray computed tomography (FXCT) using a large detector [5–8], which can reveal the distribution of inner element of object, were developed. Especially, FXCT has a highly efficient system for detecting the excited fluorescent X-rays compared to the tomographic approaches since the FXCT system does not require intense collimation in detection site. Using a detector with high efficiency and high count-rate capability [9], we have implemented FXCT with high spatial resolution in the order of tens of micrometers, and applied it to predict the effectiveness of ^{131}I therapy in hyperthyroidism because the cross sectional distribution of endogenous iodine within the thyroid could be depicted quantitatively. In this paper, FXCT images of human thyroid obtained at 0.05 mm spatial resolution with 0.05 mm slice thickness are described.

2. Methods and materials

The experiment was carried out at the bending magnet beam line NE-5A of the Tristan

*Corresponding author. Tel.: 81-298-53-3774; fax: 81-298-53-3658.
E-mail address: ttakeda@md.tsukuba.ac.jp (T. Takeda).

0168-9002/01/$ - see front matter
PII: S0168-9002(01)00654-4

accumulation ring in Tsukuba, Japan. The photon flux rate in front of the object was approximately 7×10^7 photons/mm^2/sec at a beam current of 30 mA with 6.5 GeV energy.

2.1. FXCT system

The FXCT system consisted of a silicon (1 1 1) double crystal monochromator, an X-ray slit system, a scanning table, a fluorescent X-ray detector with its X-ray collimator, a transmission X-ray detector with its rotating X-ray shutter and a pin diode (Fig. 1). The white X-ray beam was monochromatized at 37 keV X-ray energy. The monochromatized X-rays were collimated into a 0.05×0.05 mm^2 pencil beam (horizontal and vertical, respectively). Fluorescent X-rays, which are emitted isotropically from the subject along the path of the incident X-ray beam, were detected in a high purity germanium (HPGe) detector. To reduce the amount of stray radiation reaching the detector, HPGe detector was positioned perpendicular to the incident monochromatic X-ray beam, and masked by a lead collimator with 20 mm thick and its aperture 1 mm high and 30 mm wide. The distance between the HPGe detector and the specimen was 45 mm. The data acquisition time of the HPGe detector was 5 s for each scanning step. Projection data was acquired by 0.05 mm translational and 3° rotational steps over 180°. The net counts of the Kα fluorescent X-ray spectral lines at each projection were used to generate a FXCT image.

The transmission X-ray beam was measured simultaneously by a water-cooled X-ray CCD detector. The data acquisition time was 5 s at each scanning step. Transmission X-ray CT images were reconstructed by using a filtered back-projection method. The X-ray fluorescent data were corrected for the attenuation of the incident beam and the emitted fluorescent X-ray, using the attenuation information from the transmission X-ray CT image data. FXCT images were reconstructed from an algebraic method that includes the attenuation correction using a least-squares method [10]. The X-ray dose was about 2.6×10^6 photons/voxel.

2.2. Objects

The objects were 2 mm in diameter column samples of hyperthyroidism and a normal thyroid tissue fixed in 10% formalin. Phantom filled by iodine solution was measured to confirm quantitative estimation for the iodine content of the thyroid. After FXCT image was acquired, pathological

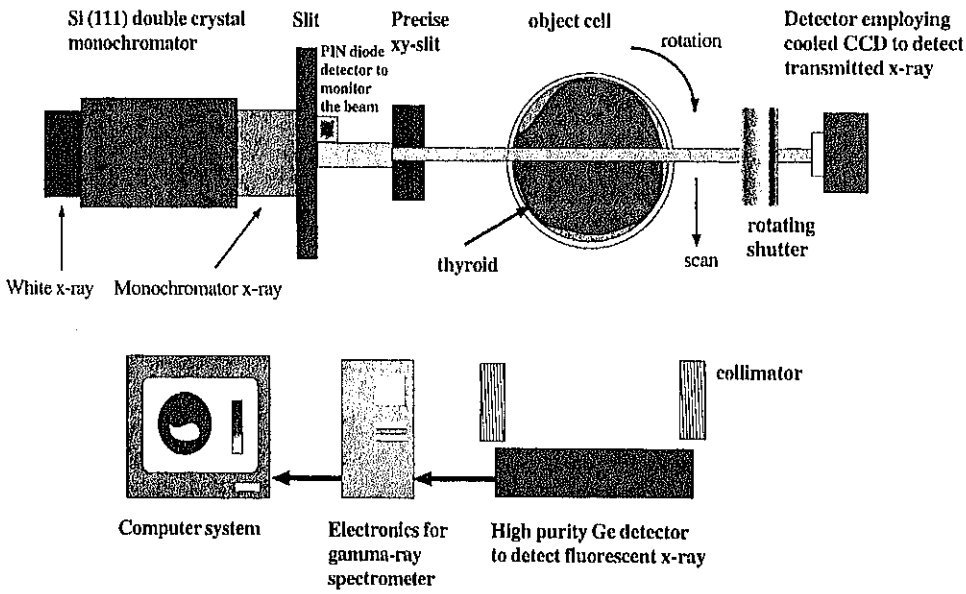

Fig. 1. Fluorescent X-ray CT system.

specimens were sliced into 0.01 mm thick and Hematoxylin–Eosin staining was performed.

3. Results and discussions

The spectrum of fluorescent Kα line was observed clearly in normal thyroid (Fig. 2). The cross sectional distribution of endogenous iodine within thyroid was clearly imaged by FXCT at a 0.05 mm in-plane spatial resolution and 0.05 mm slice thickness (Fig. 3). Here, the spatial resolution is estimated 0.054 mm by half width of point spread function obtained by cell boundary. In thyroid of normal and hyperthyroidism, the region with high iodine content revealed by FXCT corresponded to the follicles containing iodine shown by optical pictures, whereas a part of low and/or defect iodine distribution area corresponded to the vessels and connective tissues. The endogenous iodine content within the thyroid could be depicted quantitatively by FXCT, and it's content in the hyperthyroidism, which made poor FXCT image due to low signal-to-noise ratio (SNR), was 1/6 of that of normal thyroid. Thus, the effectiveness of ^{131}I therapy in hyperthyroidism [11,12] might be evaluated.

Partial and incomplete correspondence was observed between FXCT and microscopic picture, this might be caused by the difference of the cutting angle of pathological specimen, the slice thickness between FXCT (0.05 mm) and microscopy (0.01 mm), and the destruction of follicle by preparation procedure of sample. But non-destructive procedure of FXCT allows in situ observation of object. Three-dimensional (3D) FXCT might be helpful to understand the distribution of iodine and surrounding structures such as vessels and connective tissue because the network structures of vessels will be estimated. However, to understand the exact meaning of FXCT image, a combined analysis using both

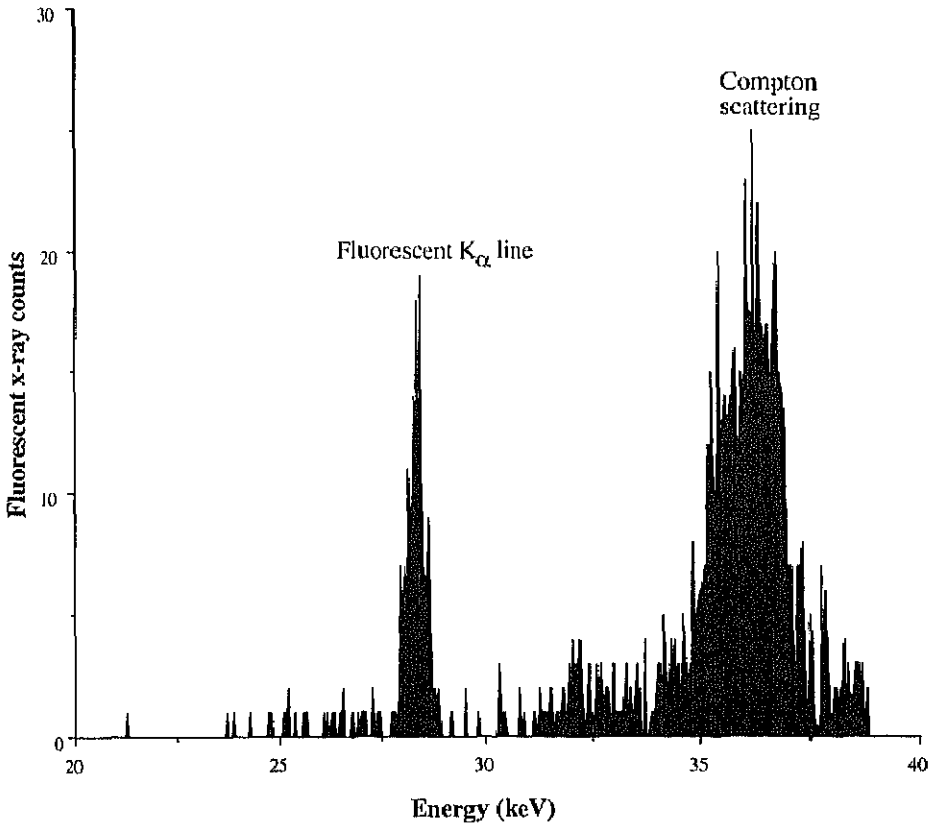

Fig. 2. Spectrum of fluorescent X-ray CT in normal thyroid obtained by a single scanning step.

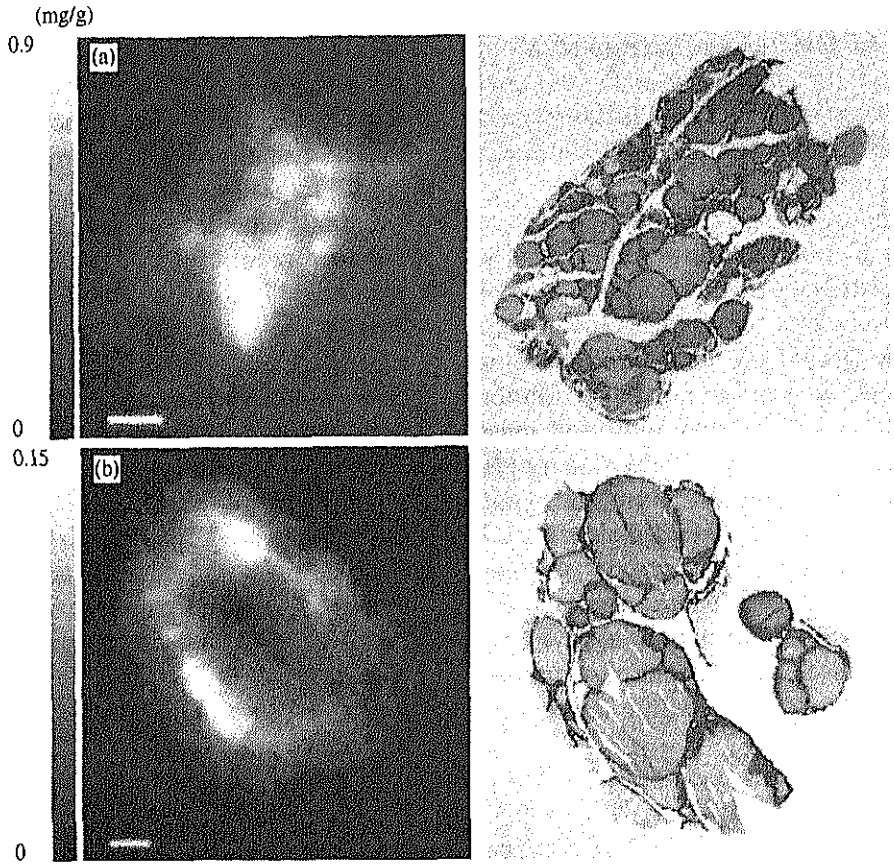

Fig. 3. Fluorescent X-ray CT image of thyroid gland obtained at 0.05 mm in-plane spatial resolution and 0.05 mm slice thickness, and optical microscopic images of corresponding slices (Hematoxylin–Eosin stain; original magnification × 20). Normal thyroid (a) and hyperthyroidism (b). Bar scale is 0.3 mm.

FXCT and optical image is necessary to differentiate various organs or tissues not including iodine.

To obtain the 3D image, high-speed image acquisition system must be developed using a detector with much high efficiency and high count-rate capability. In addition, the insertion device and/or the focusing type of apparatus [13] which increase the incident monochromatic X-rays, might be needed to improve the SNR of FXCT image and to decrease the image acquisition time.

Acknowledgements

We would like to thank Mr. K. Kobayashi for his preparation of experimental apparatus. This research was partially supported by a Grant-In-Aid for Scientific Research (No. 10557084) from the Japanese Ministry of Education, Science and Culture.

References

[1] A. Iida, Y. Gohshi, in: S. Ebashi, M. Koch, E. Rubenstein (Eds.), Handbook on Synchrotron Radiation, Vol. 4, Elsevier Publisher, Amsterdam, 1991, pp. 307.
[2] P. Boisseau, L. Grodzins, Hyperfine Interact. 33 (1987) 283.
[3] T. Takeda et al., Rev. Sci. Instr. 66 (1995) 1471.
[4] T. Takeda et al., Med. Imag. Technol. 14 (1996) 183.
[5] T. Takeda et al., SPIE 2708 (1996) 685.
[6] G.F. Rust, J. Weigelt, IEEE Trans. Nucl. Sci. 45 (1998) 75.
[7] T. Takeda et al., SPIE 3772 (1999) 258.
[8] T. Takeda et al., Cell. Mol. Biol. 46 (2000) 1077.
[9] Q. Yu et al., Med. Imag. Technol. 18 (2000) 805.
[10] T. Yuasa et al., IEEE Trans. Nucl. Sci. 44 (1997) 54.
[11] P.B. Hoffer et al., Radiology 99 (1971) 117.
[12] W.H. Beirwaltes, Semin. Nucl. Med. 8 (1978) 95.
[13] A. Simionvici et al., SPIE 3772 (1999) 304.